C. P. No. 609

C. P. No. 609

MINISTRY OF AVIATION

AERONAUTICAL RESEARCH COUNCIL

CURRENT PAPERS

Some Three-Dimensional Effects of Rotating Stall

By

S.L. Dixon,

Department of Mechanical Engineering,

Liverpool University

LONDON: HER MAJESTY'S STATIONERY OFFICE

1962

Price 5s 6d net

C.P. No.609

Some Three-Dimensional Effects of Rotating Stall

- By -
S. L. Dixon,
Dept. of Mechanical Engineering,
Liverpool University

May, 1961

SUMMARY

A small perturbation analysis of rotating stall in inviscid, incompressible flow is developed from an analysis of Yeh. An isolated blade row is considered having a blade height which is not small compared to the mean radius. A criterion is derived for the occurrence of rotating stall, the speed of stall propagation and the possible number of stall cells involved. From this the frequency of circumferential flow disturbances can be obtained. An example is given of an application of the analysis.

The main assumptions made are that a large number of small amplitude stall cells are induced at onset of stall, that the radial shift of the streamlines is small and that the absolute exit flow angle is small.

Possible explanations are suggested for the observed changes in number of stall cells.

List of Contents

5./

Previously issued as A.R.C.22,863.

---

1. Introduction

1.1 Brief summary of some experimental observations

When the flow through a compressor blade row is decreased at constant speed of rotation the angle of attack of the blades increases and the blades eventually stall. It is observed, however, that not all the blades stall simultaneously but that only a fraction of them are involved. There may be several stalled patches of blades which, moreover, are found generally to be travelling steadily around the circumference at an appreciable fraction of the blade speed. The term "rotating stall", or "propagating stall", originates from this behaviour.

The mechanism whereby the stall propagates along the row has a qualitative explanation. Consider the blades to be operating close to the point of stall and that a small disturbance initiates stall on one or two blades. The stalled passages offer a smaller area to the flow through the blades causing the approaching flow to be diverted to either side of the stall patch, as shown in the accompanying sketch.

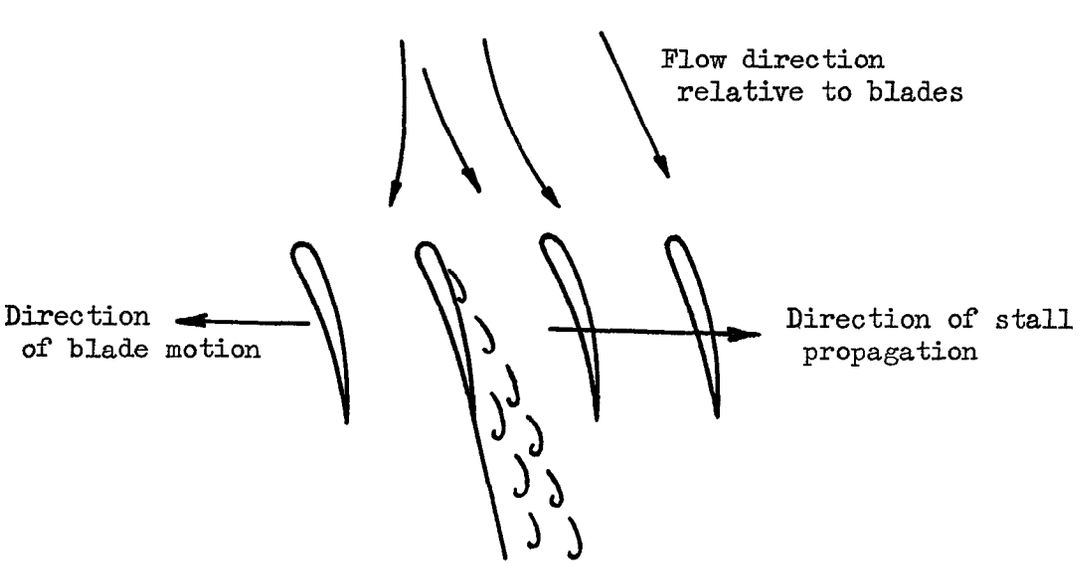

The/

The increased incidence on one side of the stall patch causes adjacent blades to stall; conversely blades stalled on the opposite side of the patch tend to become unstalled. The stall patch therefore remains a definite length, usually moving steadily* around the blades.

It is widely acknowledged that the stall cells proceed in the direction of the tangential component of the relative inlet velocity. It is possible by means of suitable inlet guide vanes to cause the stall to become stationary relative to the casing and even propagate with absolute velocity in the direction opposite to the blades (Stenning et al, Ref.2).

1.1.1 Stall patterns observed in rotor rows

Because interference between adjacent blade rows appears to have a significant effect on stall patterns produced (see Wood, Horlock and Armstrong[3]), only isolated rotor** stall patterns are considered.

Two main types of stall pattern emerge when stall is first initiated. The first type, which seems to be the most common, has been observed by Wood et al[3], Carmichael[4], Montgomery and Braun[5] and others; the pattern consists of a single stall cell which usually splits progressively into two, three and then four cells with throttling. The second type of pattern commences, with several stall cells*** which may increase in number with continued throttling and then collapse into one cell. This cell may then split into two and then three cells with further closure of the throttle. Kriebel, Seidel and Schwind[8] found that rotating stall always commenced with two cells and that opening the throttle this would change to a single cell pattern. However, they found that any slight asymmetry of the flow resulted in a single stall cell at stall initiation. The mechanism which determines the type of stall pattern developed initially and its subsequent behaviour still remains to be clarified.

The experimental observations of Rocket[1] are particularly interesting. The test rig he used had a smooth inlet passage to the rotor row, entirely unobstructed by inlet guide vanes or struts, etc. The stator row was six chord lengths downstream of the rotor.

Rocket found three stall cells at stall initiation. On opening the throttle at constant rotor speed the number of cells was reduced until only one remained. This condition was maintained indefinitely; for the same throttle setting the unstalled condition was also indefinitely maintained. Closing the throttle after stall initiation caused the number of stall cells to increase. The maximum number of cells which the rotor can maintain has not yet been determined; Emmons et al[8] suggests that with a smooth unobstructed casing the rotor might exhibit as many as one stall cell for every three blades. Continued throttling resulted in

some/

---

*Rocket[1] has reported finding a low-frequency oscillation of the cell-spacing. This oscillation was a transient condition, lasting only a few seconds, but reappearing at frequent intervals; the amplitude was sufficiently large to interfere with accurate stall velocity measurements.

**Some of the "isolated rotor" tests involved the use of guide vanes, albeit several axial chord lengths upstream!

***Stenning, Kriebel and Montgomery[6] found eight or nine, Costilow and Huppert[7] found two and Rocket[1] observed three cells at stall initiation.

some amalgamation into fewer cells (having a somewhat different nature from the earlier type) until a single large cell was formed. Reverse flow has been found in this large type of cell; a static pressure drop was observed across some of the passages with air passing upstream in those passages.

1.2 Small perturbation theories

Many theories have been advanced to determine the speed of stall propagation, the cell spacing and stall size. It is important that such a theory predicts both the propagation speed and number of stall cells around the annulus, since the product then gives the frequency of the oscillating loads imposed on the blades. The compressor designer would then be able to determine whether blade resonance is likely, leading to blade failure.

Some degree of success has been reported in determining, approximately, the stall speed; prediction of the number of stall cells for a given flow condition still remains one of the major unsolved problems of rotating stall research.

Theoretical studies of rotating stall have mostly been attempted using small perturbation theory* in which the equations of motion are linearised. These analyses are then strictly valid only for small velocity perturbations about a mean flow condition; however, the pressure rise (or deflection) need not be small**.

1.2.1 Some observed small amplitude disturbances

The amplitude of the velocity disturbances, in contrast with the assumption of small perturbation analysis, has been found to be usually of the same order of magnitude as the mean stream velocity. Small amplitude disturbances have in fact, been observed. Rannie and Marble[9] report that Benenson at California Institute of Technology was the first to find a clear example of a small disturbance propagating stall. He made observations of an annular stator cascade of hub-tip ratio 0.8 with blade solidity of about unity and found a disturbance near the cascade with velocity fluctuations of 7 to 10% of the mean stream velocity. The disturbance upstream was approximately sinusoidal, of wavelength equal to the annulus circumference. Benenson found another example of small amplitude self-induced disturbances in an isolated stator blade row in a compressor with a hub-tip ratio of 0.6. The disturbance amplitude was again 7 to 10% of the mean velocity. There were seven or eight sinusoidal waves around the annulus which, apparently, were somewhat irregular.

There appears to be no evidence that the small amplitude disturbance represents the beginning of a large amplitude disturbance.

1.2.2. Flow models used in earlier analyses

The results of any small perturbation analysis depend largely upon the assumptions made with regard to:

(i) the form of the cascade characteristics,

(ii) the nature of the downstream flow field,

(iii) certain geometrical parameters such as blade chord, circumference of blade row, hub-tip ratio etc.

Nearly/

---

*Another type of analysis based upon the vortices shed by the blade row has been used by some workers.

**The analyses of both Sears[10] and Marble[11], summarised below, were restricted to a small turning angle through the cascade.

Nearly all the analyses utilise an infinite actuator strip or an infinite blade row as the flow model; the circumference is introduced later, in some cases, as a constraint on possible wavelengths. The three-dimensional effects likely to be of importance in blade rows with low hub-tip ratios are not considered in any of the theories.

Some recent work by Yeh[12], also using a small perturbation analysis applied to an infinite actuator strip, suggested to the present writer a method whereby the number of stall cells around an annulus of low hub-tip ratio might be determined. Both the spanwise and circumferential distances are found to be of importance in obtaining possible solutions to the number of stall cells.

An outline is given below of some earlier small perturbation theories leading to Yeh's analysis; this is followed by a brief account of the differences between the present analysis and that of Yeh.

Emmons et al[13], produced the first analysis of the problem; it was shown that the cascade could be represented by a series of parallel passages, with variable outlet areas to represent the blockage effect of the stall cell. The stability of small upstream disturbances was investigated; if a critical value of the effective outlet area derivative with respect to angle of attack was attained then the disturbances could propagate unchanged along the cascade. For lower values the disturbance was attenuated, for higher values the disturbance was amplified. Emmons assumed that a blockage coefficient had been determined by experiment and that an arbitrarily assumed time delay between changes in angle of attack and blockage coefficient governed the speed of stall propagation. Emmons made no attempt to predict the velocity of stall propagation.

Sears[10] considered the case of disturbances which were large with respect to the blade chord. He assumed stall cells to exist, moving with steady velocity along the cascade, and calculated their velocity and the conditions required to produce them. The velocity field downstream of the cascade was assumed continuous so that mixing of separated and normal flow was completed in a very short distance. Sears introduced a so-called "boundary-layer phase lag" which he believed to be of major importance in determining the stall speed. This idea receives its support from experiments on single oscillating aerofoils; a phase lag is found between the coefficient of lift and angle of attack which is insensitive to frequency and is of the right order of magnitude to explain stall propagation. If this is the main controlling factor then removal of every second blade should result in doubling the speed of stall propagation. According to Iura and Rannie[14] no such large change has been observed; however, Stenning[6] using a stationary circular cascade with outward radial flow has found there is a tendency for the stall speed to increase with decreasing solidity*.

It is of interest to note that Sears obtained a solution showing stall propagation occurring even with zero phase lag.

A further questionable assumption concerns the cascade characteristic. This was represented as a continuous function of inlet angle with zero average pressure rise across the blade row during stall propagation. Rotating stall commences, in many cases, just after the peak pressure rise.

Marble[11] rejected the boundary phase-lag used by Sears and considered the inertia of the fluid outside the cascade as controlling the stall phenomenon. Attention was concentrated on the variation of static pressure rise as the cascade approached stall. According to Marble, at

stall/

---

*For the solidities normally used in compressor blade rows this effect appears to be negligible.

stall the static pressure rise decreased to zero, and remains so for all higher incidences, the turning angle being virtually unaffected. There is therefore a discontinuity in static pressure at cascade inlet resembling a square wave. Marble then showed that the imaginary part of the complex function representing a source at the origin has a discontinuity close to the origin. By combining the imaginary parts of an infinite row of sources and sinks a model was established to present the static pressure distribution. The velocity perturbations associated with this distribution of static pressure must induce flow incidences sufficient to stall the blades at one end of a stall cell and to unstall them at the other. By satisfying these conditions the angular speed of stall propagation, the extent of the stalled region and its dependence upon operating conditions together with the pressure loss due to stall, may be deduced. The velocity of stall is the same as Sears' value with zero phase lag.

Agreement was shown between the theory and an experimental value of the propagation speed measured in a compressor. Marble considered this fortuitous although Wood[15] thought it possible that the disturbances caused by stall were actually small so giving the close correlation between theory and experiment.

Stenning[16] extended the theory of Emmons and obtained the velocity of stall propagation in terms of the air angles, disturbance wavelengths and static pressure rise coefficient. In a further analysis[6] the theory was developed to include boundary-layer effects. Briefly, Stenning assumed that the stall cells produce regions of flow separation which do not mix with the downstream flow. The wake behind the cascade then consists of a number of free jets discharging into a region of constant pressure. Conditions downstream of the cascade are thereby ignored; a solution is obtained for a stability criterion and stall speed by equating a perturbation potential function derived for the cascade entry with its equivalent for the upstream flow field.

The expression derived by Stenning for stall speed implies that only pure sinusoidal disturbances traverse the cascade since the velocity depends on wavelength and harmonics would travel at speeds different from the fundamental. Stenning and Wood[15], considered the analysis inadequate in this respect and not in agreement with observations. Other criticisms which have been levelled at this analysis are:

(i) The stability criterion and speed of stall propagation can only be determined <u>after</u> measurement of the disturbance wavelength.

(ii) Numerous observations (including those of Stenning) have shown that pressure fluctuations occur in the downstream field.

In an Appendix to his paper, Stenning considered an alternative assumption where the fluid from each blade passage mixed without pressure recovery immediately after leaving the cascade. The downstream flow field is then a continuum. The true condition lies between this extreme and that of the free jets discharging into region of constant pressure and, according to Stenning will be closer to one or the other depending on the relative size of stall region to that of the blade chord.

For the assumption of zero pressure recovery Stenning obtained a solution for stall speed; for large wavelengths and zero pressure rise coefficient this reduces to the Sears-Marble result.

Wood[15] made similar assumptions to Emmons and Stenning but considered the blade chords to be small compared with the wavelength disturbance. As a result the propagation speed was found to be independent of frequency. The effect of the boundary-layer time delay was also considered (in the manner of Stenning) and found by Wood to decrease the propagation speed.

Similar/

Similar analyses using small perturbation theory have been made by Whitehead[17] and Rannie and Marble[9].

1.2.3 Yeh's analysis

The small perturbation analysis used by Yeh[12], with an infinite actuator strip of finite span, considered the general case of flow with a small stationary inlet velocity distortion and the effect of the actuator on the resulting small stationary outlet distortion.

Because of the linearisation of the steady equations of motion, the distortion can be separated from the actuator induced disturbances; the latter can then be expressed by a steady potential function in terms of wave numbers related to the blade span and a "circumferential" distance. By using the continuity condition across the actuator together with the assumption that the distortion velocity remains parallel to the main flow, Yeh related the cascade characteristics (flow angles and pressure losses) and found the ratio of outlet to inlet distortion velocities. For the case when the inlet distortion vanishes, he showed that the outlet distortion could still exist under certain necessary conditions and that this self-induced distortion could be of two basic types. These are a purely spanwise (stationary) distortion and a travelling distortion having both "circumferential" and spanwise effects. So that the steady equations of motion, in the latter case, were still applicable it was necessary at this stage for Yeh to refer his co-ordinate system relative to the distortion.

Yeh then compared the conditions under which the circumferential plus spanwise distortion could occur with that of the special case of a purely circumferential distortion, from which he deduced that the latter type always occurred first. This inference appears to be founded on the belief that the specific wave numbers chosen for the comparison are representative of all cases. This is not so and it is shown later that rotating stall without spanwise effects occurs only exceptionally; the combined spanwise plus circumferential distortion appears to be the rule. The purely spanwise axisymmetric distortion was shown by Yeh to be unlikely to occur before other stall modes.

The speed of stall propagation resulting from the simplified analysis, involving as it does only a purely circumferential distortion, has been compared by Yeh with experimental data. Relatively few results can be compared since the analysis applies only to an isolated actuator with the distortion limited strictly to a small amplitude. The ratio

$k = \dfrac{\text{stall speed relative to blades}}{\text{axial velocity}}$ found by Yeh is,

$$k = \frac{(1 + \bar{N})}{2 \cos^2 \beta_2 \cdot \tan \beta_1}$$

where $\bar{N} = \dfrac{\Delta\beta_2}{\Delta\beta_1}$

β_1 = inlet angle relative to blades

β_2 = outlet angle relative to blades.

The data used by Yeh and the above correlation (Fig.18, Ref.12) are shown in Fig.2; it would seem that the above prediction is reasonably followed.

1.3/

1.3 The present analysis

In the front stages of compressors where low hub-tip ratios are normal, three-dimensional effects are likely to be important. The present writer has approached the problem of small amplitude rotating stall in relation to the isolated stator of a moderately low hub-tip ratio compressor stage. Some of Yeh's techniques have been adopted; the following analysis differs, mainly, from that of Yeh in that:

(1) A rotating co-ordinate system has been used at the outset; the stall cells are stationary in this framework and the flow is steady.

(2) The potential function equations derived for the present low hub-tip ratio model are radically different from those of Yeh.

(3) Circumferential wavelengths are a fractional part of a circumference.

(4) The distortion involves both spanwise and circumferential effects.

(5) The conditions under which the potential solutions are valid are rather restricted; it is necessary that there be a large number of stall cells, that the disturbance is small, that there is little radial shift of the streamlines, and that the absolute exit flow angle is small. (See Appendix I.)

2. Description of the Flow Model

Consider an actuator disc, having an infinite number of infinitesimally small blades, whose axis is coincident with the axis of a circular annular passage of uniform section. The axis of the passage represents the x direction extending from $-\infty$ upstream to ∞ downstream. The disc is located at $x = 0$. Any fixed point within the annular passage may be described by means of a system of orthogonal cylindrical co-ordinates (x, r, θ) as in Fig.1(a). The inner and outer radii of the annulus are denoted by r_i and r_o respectively.

The components of the absolute undistorted velocity are denoted by $U = U(r)$ parallel to the axis and $V = V(r)$ circumferentially. Since the flow is considered to be in radial equilibrium at the stations $x = \pm\infty$, in general the axial component U of the main flow will be dependent upon radial position. The absolute flow angle, β, is

$$\beta(r) = \tan^{-1} \frac{V(r)}{U(r)} .$$

A pattern of stall cells of small amplitude is imagined to be rotating around the annulus at a uniform speed, kU. The pattern of cells is at a fixed radius and radially of small extent; it will strictly be an incipient stall.

By taking the reference frame as fixed within the pattern of stall cells, the problem may be reduced to one of steady flow. Representing the main flow tangential velocity component, relative to the stall pattern, by V^*, the main flow angle relative to stall β^*, is

β^*/

$$\beta^* = \tan^{-1}\left(\frac{V^*}{U}\right)$$

and as

$$\beta = \tan^{-1}\left(\frac{kU + V^*}{U}\right)$$

then

$$\tan\beta = k + \tan\beta^*.$$

The relative position of the various angles is clear from Fig.1(a).

2.1 The induced velocities

The actuator disc induces a perturbation of the velocity fields which has velocity components, relative to the stall pattern, of

$$w_x = w_x(x, \theta, r)$$

$$w_\theta = w_\theta(x, \theta, r)$$

$$w_r = w_r(x, \theta, r)$$

in the axial, tangential and radial directions respectively.

Now a rotating stall is essentially a self-induced phenomenon; it is represented in this analysis by a velocity distortion of the downstream field generated in the actuator disc plane. There is no distortion of the upstream field due to the stall. The generated distortion is assumed to be convected downstream along the flow lines at the angle β_2^* relative to the stall cells. (i.e., at the flow angle, relative to the stall, at ∞ downstream.) It is shown in Appendix I that the amplitude of this distortion is necessarily very small compared with the main velocity components.

The axial and tangential components of the stall velocity distortion are respectively,

$$\Delta U = \Delta U(x \tan\beta_2^* - r\theta, r)$$

$$\Delta V = \Delta V(x \tan\beta_2^* - r\theta, r) .$$

The first parameter $(x \tan\beta_2^* - r\theta)$ expresses the dependence of ΔU and ΔV on the flow line considered (at a constant radius); the second parameter some dependence on r.

Sketch/

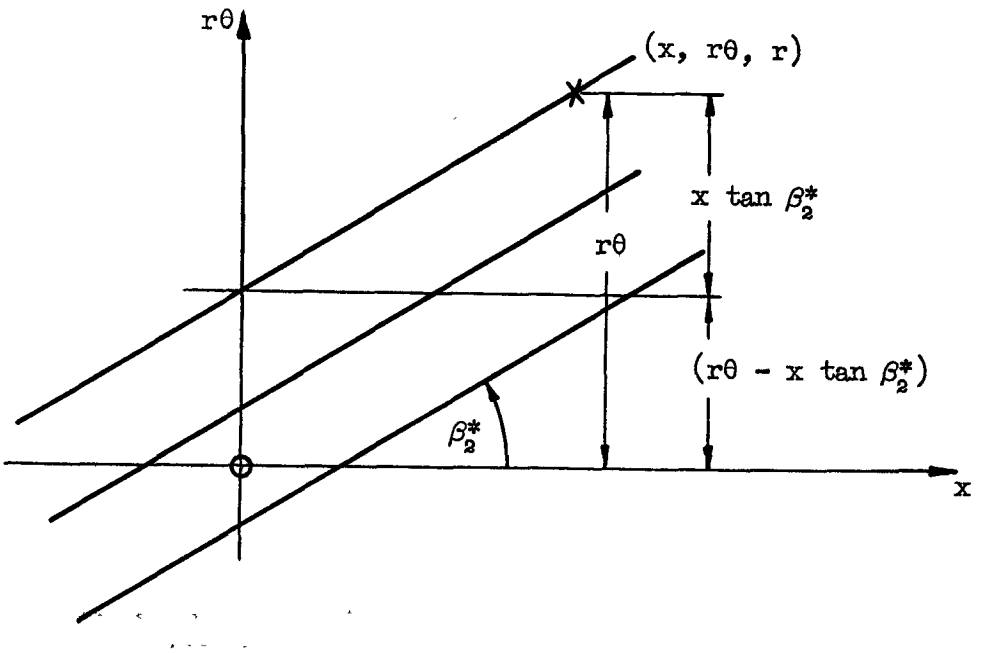

The sum of all the various components of velocity relative to the stall in the axial, tangential and radial directions are, respectively,

$$U(r) + \Delta U(x \tan \beta_2^* - r\theta,\ r) + w_x(x,\ r,\ \theta)$$

$$V^*(r) + \Delta V(x \tan \beta_2^* - r\theta,\ r) + w_\theta(x,\ r,\ \theta)$$

$$w_r(x,\ r,\ \theta)\ .$$

These are the velocity components of the <u>downstream</u> flow field; upstream of the actuator disc the ΔU and ΔV components vanish (i.e., there is no inlet disturbance).

3. <u>Analysis</u>

The continuity equation applied to the steady flow model (i.e., relative to the stall pattern) for "incompressible" or low Mach number flow is,

$$\frac{\partial}{\partial x}(U + \Delta U + w_x) + \frac{1}{r}\frac{\partial}{\partial \theta}(V^* + \Delta V + w_\theta) + \frac{1}{r}\frac{\partial}{\partial r}(r\, w_r) = 0$$

or $$\frac{\partial w_x}{\partial x} + \frac{1}{r}\frac{\partial w_\theta}{\partial \theta} + \frac{1}{r}\frac{\partial}{\partial r}(r\, w_r) + \frac{\partial \Delta U}{\partial x} + \frac{1}{r}\frac{\partial}{\partial \theta}\Delta V = 0$$

as, in general, $U = U(r)$ and $V^* = V^*(r)$ only.

Now $$\frac{\partial \Delta U}{\partial x} = \frac{\partial \Delta U}{\partial (x \tan \beta_2^* - r\theta)} \cdot \tan \beta_2^*$$

and $$\frac{1}{r}\frac{\partial \Delta V}{\partial \theta} = \frac{-\partial \Delta V}{\partial (x \tan \beta_2^* - r\theta)}\ .$$

The assumption that the distortion remains parallel to the relative main flow and is unaffected by the velocity perturbations of the actuator disc, gives,

$\Delta V/$

$$\Delta V = \tan \beta_2^* \cdot \Delta U \qquad \ldots (1)$$

where β_2^* is constant at a given radius.

Then, $$\frac{\partial \Delta U}{\partial x} + \frac{1}{r}\frac{\partial \Delta V}{\partial \theta} = \frac{\partial \Delta U}{\partial (x \tan \beta_2^* - r\theta)} \cdot \tan \beta_2^* - \frac{\partial \Delta V}{\partial (x \tan \beta_2^* - r\theta)} = 0$$

The continuity equation is now reduced to

$$\frac{\partial w_x}{\partial x} + \frac{1}{r}\frac{\partial w_\theta}{\partial \theta} + \frac{1}{r}\frac{\partial}{\partial r}(r\, w_r) = 0 . \qquad \ldots (2)$$

Considering only the relative perturbation velocities; these are zero at $x = \pm \infty$ and their vorticity components are likewise zero. Since the fluid is assumed inviscid the vorticity due to the perturbation velocities, by Kelvin's theorem, is everywhere zero. (See Appendix I on the conditions necessary for perturbation potential flow of the downstream field.) A potential function Φ is defined such that,

$$w_x = \frac{\partial \Phi}{\partial x}, \quad w_\theta = \frac{1}{r}\frac{\partial \Phi}{\partial \theta}, \quad w_r = \frac{\partial \Phi}{\partial r} .$$

Equation (2) can now be written

$$\frac{\partial^2 \Phi}{\partial r^2} + \frac{1}{r}\frac{\partial \Phi}{\partial r} + \frac{1}{r^2}\frac{\partial^2 \Phi}{\partial \theta^2} + \frac{\partial^2 \Phi}{\partial x^2} = 0 .$$

This equation may be solved by the usual process of separating the variables. The form of the solution is largely determined by the boundary conditions to be satisfied. These are briefly; the induced perturbation velocities vanish at $\pm \infty$; the radial velocity vanishes on the annulus walls; the tangential velocity perturbation is periodic; for the single wave analysis it is assumed sinusoidal.

The potential solutions for a single wave are,

$$\left.\begin{aligned} \Phi_1 &= A_{m,n}\, e^{mx+in\theta}\,[J_n(mr) + B_{m,n}\, Y_n(mr)] \\ \Phi_2 &= C_{m,n}\, e^{-mx+in\theta}\,[J_n(mr) + D_{m,n}\, Y_n(mr)] \end{aligned}\right\} \qquad \ldots (3)$$

Φ_1 applies to the upstream region and Φ_2 to the downstream region. $J_n(mr)$, $Y_n(mr)$ are ordinary Bessel functions of the first and second kind respectively of order n and argument mr.

$A_{m,n}$, $B_{m,n}$, etc., are constants related to particular values of m and n.

If L_θ is half the wavelength of the circumferential oscillation, then

$$n = \frac{\pi r}{L_\theta} .$$

That/

That is, at any radius r, it is supposed that only an integral number of waves n, can be contained around the circle of length $2\pi r$.

Observing the radial boundary conditions, $w_r = 0$ at $r = r_i$ and $r = r_o$, then

$$\frac{J_n'(m\,r_i)}{Y_n'(m\,r_i)} - \frac{J_n'(m\,r_o)}{Y_n'(m\,r_o)} = 0 \qquad \ldots (4)$$

where $'$ denotes differentiation with respect to r. Hence for a given ratio of hub-tip radii, solutions may be found to the above Bessel function boundary equation in terms of the numbers m and n. These are examined in detail in Section 5.2.

Two important relations can be found from the potential functions, equations (3). Denoting hereafter, conditions immediately upstream and downstream of the actuator plane by suffixes 1 and 2 respectively then,

$$\left.\begin{aligned} w_{\theta_1} &= iqw_{x_1} \\ w_{\theta_2} &= -iqw_{x_2} \end{aligned}\right\} \qquad \ldots (5)$$

where $$q = \frac{n}{mr}.$$

Applying the continuity equation to the flow across the actuator disc, we have, noting that there is no disturbance velocity component upstream of the actuator,

$$w_{x_1} = w_{x_2} + \Delta U. \qquad \ldots (6)$$

4. The Cascade Characteristics

The steady flow through a cascade section of any given geometry, in terms of the inlet flow angle β_1, is fully determined by any pair of independent flow parameters. The two parameters most frequently used, as in the following are,

(i) the exit flow angle β_2,

(ii) the loss in total pressure.

With stall of small amplitude propagating around the cascade, the flow relative to the blades is essentially unsteady. The problem is reduced to one of steady motion by fixing the reference frame in the rotating stall.

4.1 Flow angles

Considering first the exit flow angle β_2. For small flow variations,

$$\Delta\beta_2 = \bar{N} \cdot \Delta\beta_1,$$

where $\bar{N}$ is a constant equal to the slope of the β_2 versus β_1 curve at the cascade operating point.

Now/

Now $$\tan(\beta + \Delta\beta) = \frac{U \tan\beta + \Delta V + w_\theta}{U + \Delta U + w_x}$$

$$\therefore \Delta \tan\beta = \frac{\Delta V + w_\theta}{U} - \frac{\tan\beta}{U}(\Delta U + w_x) = \sec^2\beta \cdot \Delta\beta$$

$$\therefore \Delta\beta = \frac{\cos^2\beta}{U}\{(\Delta V + w_\theta) - \tan\beta\,(\Delta U + w_x)\} . \qquad \ldots (7)$$

Hence $$(\Delta V + w_{\theta_2}) - (\Delta U + w_{x_2}) \tan\beta_2 = N[w_{\theta_1} - w_{x_1} \tan\beta_1] , \qquad \ldots (7a)$$

where $$N = \frac{\bar{N}\cos^2\beta_1}{\cos^2\beta_2} = \frac{\Delta \tan\beta_2}{\Delta \tan\beta_1} . \qquad \ldots (8)$$

Using equation (5), equation (7a) becomes

$$(\Delta U \tan\beta_2 - \Delta V) + w_{x_2}(\tan\beta_2 + iq) = w_{x_1} N(\tan\beta_1 - iq) \qquad \ldots (9)$$

4.2 Pressure losses

With P_t for undisturbed total pressure and p_t for perturbation total pressure, then

$$P_t + p_t = P + p + \frac{\rho}{2}[(U+\Delta U+w_x)^2 + (V^*+\Delta V+w_\theta+kU)^2]$$

$$\doteq P + p + \frac{\rho}{2}[U^2 + (kU+V^*)^2] + \rho[U(\Delta U+w_x) + (V^*+kU)(\Delta V+w_\theta)] .$$

Now $$P_t = P + \frac{\rho}{2}[U^2 + (kU+V^*)^2] , \quad \text{by definition}$$

$$\therefore p_t = p + \rho[U(\Delta U+w_x) + (V^*+kU)(\Delta V+w_\theta)] .$$

To the first order, the equation of motion in the axial direction is

$$U\frac{\partial w_x}{\partial x} + \frac{V^*}{r}\frac{\partial w_x}{\partial \theta} = -\frac{1}{\rho}\frac{\partial p}{\partial x} . \qquad \text{(see I.3b)}$$

With the condition of irrotational perturbations,

$$\frac{1}{r}\frac{\partial w_x}{\partial \theta} = \frac{\partial w_\theta}{\partial x}$$

and the above equation becomes

$$\rho\,(U \cdot w_x + V^* \cdot w_\theta) + p = 0$$

$$\therefore p_t = \rho[U\Delta U + (V^* + kU)\Delta V + kUw_\theta] . \qquad \ldots (10)$$

The/

The loss in total pressure across the cascade for the main flow alone is,

$$P_{t_1} - P_{t_2} = \bar{\omega} \cdot \frac{\rho}{2} [U^2 + (kU + V_1^*)^2]$$

For the perturbed flow,

$$(P_{t_1} + p_{t_1}) - (P_{t_2} + p_{t_2}) = (\bar{\omega} + \Delta\bar{\omega}) \frac{\rho}{2} [(U + w_{x_1})^2 + (V_1^* + w_{\theta_1})^2]$$

where $\bar{\omega}$ is the loss coefficient for the main flow and $\Delta\bar{\omega}$ the incremental change of $\bar{\omega}$ due to a change in β_1 as a result of velocity perturbations.

Ignoring products of small quantities,

$$p_{t_1} - p_{t_2} = \frac{\rho U^2}{2} \left\{ \Delta\bar{\omega} \sec^2 \beta_1 + \frac{2\bar{\omega}}{U} (w_{x_1} + w_{\theta_1} \tan \beta_1) \right\}.$$

With $\Delta\bar{\omega} = 2M \Delta\beta_1$ and equation (7), then

$$p_{t_1} - p_{t_2} = \rho U \{M(w_{\theta_1} - w_{x_1} \tan \beta_1) + \bar{\omega} (w_{x_1} + w_{\theta_1} \tan \beta_1)\},$$

where M is a constant equal to half the slope of the $\bar{\omega}$ versus β_1 curve at the operating point of the cascade.

Using equation (10) together with equation (5) in the last expression,

$$iqk(w_{x_1} + w_{x_2}) - (\Delta U + \Delta V \tan \beta_2) = M w_{x_1} (iq - \tan \beta_1) + \bar{\omega} w_{x_1} (1 + iq \tan \beta_1). \quad (11)$$

5. Solutions

The foregoing equations (9) and (11) represent the cascade characteristics; together with the continuity relation across the actuator disc, equation (6), and the assumption that the self-induced distortion is convected at the angle β_2^* relative to stall, equation (1), it is now possible to eliminate ΔU, ΔV, w_{x_1} and w_{x_2} and solve for M and k in terms of the quantities q, $\bar{\omega}$, N and the flow angles, β_1 and β_2.

Two expressions for $w_{x_1}/\Delta U$ can be found using equations (1), (6), (9) and (11). Equating these, rearranging and separating the real and imaginary parts we have, eventually,

$$M = \frac{(1+b_2 b_2^*)(b_2 - N b_1) + (b_2^* - q^2 b_1)\bar{\omega} + q^2 k(1-N)}{b_1 b_2^* + q^2} \quad \ldots (12a)$$

and

$$M = \frac{(1+k^2+b_2^{*2}) + (1+b_2 b_2^* - k b_1)N + \bar{\omega}(1+b_1 b_2^*)}{b_1 - b_2^*} \quad \ldots (12b)$$

where for convenience, $b \equiv \tan \beta$.

Equating/

Equating (12a) and (12b), k can be found as the roots of,

$$Ek^3 + Fk^2 + Gk + H = 0 \qquad \ldots (13)$$

where $E = -2b_1$

$$F = 4b_1 b_2 + q^2(N+1) + b_2^2 + Nb_1^2 + \bar{\omega}(1+b_1^2)$$

$$G = -\{2b_2 N(q^2+b_1^2) + (b_1+b_2)(1+q^2+2b_2^2) + 2\bar{\omega}b_2(1+b_1^2)\}$$

$$H = (1+b_2^2)\{b_2^2 + Nb_1^2 + q^2(1+N)\} + \bar{\omega}(1+b_1^2)(q^2+b_2^2) \ .$$

That is, the speed of stall propagation is a function of the cascade operating point characteristics and wave parameter, q.

5.1 Evaluating M and k

When some radial section of the cascade is operating close to the "stall point", the parameter 2M is equal to the rate of change of total-pressure loss coefficient with change of inlet angle necessary for stall to propagate at that section. The speed of the stall is then kU. This "necessary M" is given the symbol M_{nec} to distinguish it from the actual value to M which can be obtained from measurements of cascade performance. The actual value of M is denoted by M_{act}. Stall will be supposed to propagate when,

$$M_{nec} = M_{act}$$

at a given radial section.

For a compressor stator it is normal to find some radial variations in the values of N, b_1 and b_2, depending upon blade design and operating condition. The application of the analysis to an actual stator, together with estimates of M_{act}, so enabling prediction to be made of the conditions under which stall first propagates, is not attempted here. It is important to find how the value of M_{nec} is influenced by the parameter q for prescribed values of b_2 and N with b_1 as independent variable.

As the calculation of k and M_{nec} proved fairly lengthy it was decided to develop a simple programme for the University's D.E.U.C.E. electronic digital computer.

Fig.3(a) shows the variation of M_{nec} with q for several values of b_1 with $N = b_2 = \bar{\omega} = 0$ and Fig.3(b) the corresponding values of the stall speed ratio, k. . The significant characteristic of Fig.3(a) is that for constant values of b_1, M_{nec} decreases to a minimum and then increases as q is increased. This characteristic is typical for a wide range of values of N and b_2. The conclusion is drawn that a blade section on the point of stalling and having specific values of b_1, b_2 and N will be most likely to stall with a value of q corresponding to the minimum of M_{nec}. The previously arbitrary nature of q is now absent, q being fixed by M_{min} (minimum for M_{nec}) for a particular b_1, b_2 and N.

Values of M_{min} are shown in Fig.4 for a wide range of values of b_1 and b_2 and for three values of N. These three N values have been chosen to represent blades having high, medium and low solidities; these are N = 0, 0.2 and 0.4 respectively. In all calculations the effect of the pressure loss coefficient $\bar{\omega}$ has been ignored. The values of k and q corresponding to the M_{min} values are shown in Figs.5(a) and 5(b) respectively.

It/

It is seen that for $N = 0.2$ and 0.4 in Fig.4 and Fig.5(a) a line is drawn to indicate $q = 0$. This line is a validity limit since, for the present analysis, no relevant meaning can be attached to values of $q^2 < 0$. (See boundary conditions related to equation (3).)

5.2 Solution of boundary equation

Equation (4) may be written,

$$f(\mu) = \frac{J_n'(\mu)}{Y_n'(\mu)} - \frac{J_n'\left(\frac{r_i}{r_o} \cdot \mu\right)}{Y_n'\left(\frac{r_i}{r_o} \cdot \mu\right)} = 0$$

where $$\mu = mr_o .$$

Using the tables of Bessel functions[18,19] the first three roots of the equation $f(\mu) = 0$ have been found for $r_i/r_o = \frac{1}{2}$ and the first and second roots for $r_i/r_o = \frac{3}{4}$; these are shown in Fig.6 in the form n/μ against n, for convenience.

Now $$q = \frac{n}{mr} , \quad \text{by definition}$$

$$\therefore q\frac{r}{r_o} = \frac{n}{\mu} .$$

For a particular blade section, r/r_o, if N and the flow angles are known, a value of q for stall propagation can be found as outlined in Section 5.1. For a given hub-tip ratio, r_i/r_o and using the above expression, values of n may then be found. Notice, however, that n is required to be an integer.

An asymptotic solution exists for the Bessel equation $f(\mu) = 0$ such that for large values of n, n/μ tends to unity for all roots (see Appendix II). At any radius, therefore, there is an upper limit to q imposed by the boundary conditions,

e.g., at $$r = r_o, \quad q \leqslant 1$$

and at $$r = r_i = \frac{r_o}{2} \text{ (say)}, \quad q \leqslant 2.$$

5.3 Effect of cascade geometry variation

It may be possible by suitable choice of cascade geometry to either increase M_{min} or to reduce the actual value of M and so delay the onset of stall. Stall is supposed to commence when the actual M, which is the measured rate of change of total pressure loss coefficient at a particular blade section, equals the value of M_{min}.

Comparing the data of Fig.4 at the same flow angles but at different values of N it will be observed that, for the range of angles chosen, M_{min} increases as N increases. If high values of N can be construed to mean lower solidity then, other things being equal, the onset

of/

of stall should be delayed by choosing lower solidity blading. There is the possibility, however, that varying the cascade geometry to provide a more favourable M_{min}, may adversely affect the actual M values.

According to the present theory $q^2 \geq 0$ to satisfy equation (3). It should not be possible for rotating stall to exist at high N values with certain combinations of b_1 and b_2 since q^2 will be less than zero.

6. Application of Solutions

The criterion for predicting the onset of rotating stall, namely $M_{act} = M_{min}$, is applied to a single isolated stator at a particular radius.

Estimates may be made, by adapting conventional techniques* (see Ref.21), of the performance of a blade row with a specified geometry. The total pressure losses and flow angles can be estimated, at a given radius, as functions of inlet angle. From this information the variation of M_{min} and M_{act} with flow coefficient is derived, their point of intersection, fixing the stall condition at this radius. This procedure may be extended to other points along the blade span and the radius found at which stall is first initiated.

6.1 Example

Suppose that an isolated stator row with a hub-tip ratio, $r_i/r_o = \frac{3}{4}$, first stalls at the tip when $b_1 = \tan \beta_1 = 1.1$, $b_2 = \tan \beta_2 = 0.1$ and

$$N = \frac{\Delta \tan \beta_2}{\Delta \tan \beta_1} = 0.2 .$$

From Fig.5(b) we obtain $q = 0.47$.

At $r = r_o$, $q \dfrac{r}{r_o} = \dfrac{n}{\mu} = 0.47$.

From Fig.6 we obtain $n = 7$ (a second root solution), i.e., 7 stall cells.

The corresponding value of $k = 0.35$ from Fig.5(a) and of $M_{min} = 0.965$ from Fig.4.

7. Discussion

The principal result of this report is that a frequency of stall propagation can be obtained for a restricted type of rotating stall. The main assumptions on which the analysis is based are:

(i) Small perturbation theory is used which limits the amplitudes of perturbation and self-induced disturbance velocities. Although most reported cases of rotating stall are known to have large amplitude disturbances some results do confirm that small amplitude disturbances can exist.

(ii)/

---

*Radial equilibrium or actuator disc techniques using Howell's cascade correlation.

(ii) Either, a large number of stall cells are formed and the absolute flow angle at exit is small (this exit flow is assumed a fairly close approximation to a free-vortex), or,

(iia) The absolute flow angle at exit is zero. This assumption is necessary for a potential solution of the downstream flow field.

(iii) Only a small radial shift of the streamlines is allowed.

(iv) The self-induced disturbances are convected at constant amplitude along the undisturbed stream-lines.

(v) The assumption that an actuator disc can replace the blade row ignores the inertia effects within the blade row.

(vi) Only an isolated stator is considered: there are no interference effects from other blade rows.

(vii) Inviscid and incompressible flow.

7.1 Changes in number of stall cells

In the example considered above, values of β_1, β_2, N and r/r_o were chosen such that n was, conveniently, an integer value. The stall criterion might have applied to slightly different conditions so that a non-integer for n was derived. It is suggested that this may give rise to the observed effect of unsteadiness in the number of stall cells under steady flow conditions. Cases of this kind are fairly common and are reported by Rocket[1], Rannie[9], Stenning[6] and others. It appears that the number of cells can remain at, say, eight for a time and for no apparent reason, suddenly change, for instance, to nine cells. An examination of Fig.3 shows that at high values of b_1 the curves of M near M_{min} are relatively flat with change of the parameter q. Small changes may occur in the value of q without appreciably altering the stall criterion, producing the observed change in number of stall cells.

A tentative explanation can be also given to the large changes reported in the number of stall cells for small changes in throttle setting. It is seen that for the same value of $q\frac{r}{r_o}$, (Fig.6) there is more than one solution for n, as there are many roots of the solution to the Bessel equation. Considering, for example, the case where the hub-tip radius ratio is 0.5, at a value of $q\frac{r}{r_o} = 0.459$ the third root gives $n = 8$. A small change of $q\frac{r}{r_o}$ to 0.45, gives a steady value of $n = 4$ for the second root.

Adequate supporting evidence for this explanation is lacking. The observed changes in number of the stall cells formed may be accompanied by changes in both propagation speed and character of the stall cells. The amplitudes of the velocity fluctuations within the cells are generally large which, strictly, invalidates the assumptions on which the theory is built.

7.2 Further work

A large size, low-speed, two-stage compressor having a hub-tip radius ratio of 0.75 has been constructed at Liverpool. All blade rows are removable and all blades can be set at varying stagger angles. The flow upstream of the stages is completely free from obstructions. With this test-rig it is hoped shortly to run a series of tests with only the inlet guide vanes and first row of rotor blades installed followed by the second row stator blades. By this means it is hoped to simulate the conditions of operation required by the analysis.

Measurements/

Measurements can be conducted, at varying throttle, of upstream and downstream total pressure and flow angles, etc. At stall initiation hot-wire anemometry can provide information on the number of stall cells, their speed of propagation and amplitude of velocity disturbances in the cells. A check can be made on the criterion of stall cell formation assuming that small amplitude velocity disturbances are involved. Whether the tests envisaged will produce such a phenomenon cannot be foreseen.

Acknowledgement

The author would like to acknowledge with gratitude the encouragement and useful suggestions of Prof. J. H. Horlock during the preparation of this report.

Symbols

b	$\tan \beta$
b^*	$\tan \beta^*$
$J_n(\mu)$, $Y_n(\mu)$	Bessel functions of first and second kind respectively, of order n and argument
k	velocity ratio (kU is velocity of stall propagation)
L_θ	half wavelength of circumferential oscillation
m	decay factor for velocity perturbations
M	$\dfrac{\Delta\bar{\omega}}{2\Delta\beta_1}$
n	number of complete circumferential waves
N	$\dfrac{\Delta \tan \beta_2}{\Delta \tan \beta_1}$
$\bar{N}$	$\dfrac{\Delta\beta_2}{\Delta\beta_1}$
p	static pressure perturbation
p_t	total pressure perturbation
P	static pressure associated with main flow
P_t	total pressure associated with main flow
q	n/mr, (a wave parameter)
r,x,θ	co-ordinates, (see Fig.1)
r_i, r_o	inner and outer radii of actuator disc
$\bar{u},\bar{v}$	axial and tangential velocity changes at $x = \pm\infty$ (see Appendix I)
U,V	main axial and tangential absolute velocities
$\Delta U, \Delta V$	axial and tangential flow distortion velocities

$\underline{w}$	vorticity vector
w_r, w_x, w_θ	velocity perturbations induced by actuator disc relative to stall
W	main flow velocity relative to stall, $\sqrt{U^2 + V^{*2}}$
β	absolute main flow angle
β^*	main flow angle relative to stall
$\Delta\beta$	change of flow angle
ζ, η, ξ	orthogonal components of vorticity along the radial, circumferential and axial directions respectively
μ	mr_o
ρ	fluid density
Φ	velocity potential
$\bar{\omega}$	total pressure loss coefficient for main flow
$\Delta\bar{\omega}$	incremental change of $\bar{\omega}$ due to change of β_1
Ω	angular velocity of rotating co-ordinate system.

References/

References

No.	Author(s)	Title, etc.
1	J. A. Rocket	Modulation phenomena in stall propagation. Trans. A.S.M.E., Vol.81, No.3, pp.417-425, September, 1959.
2	A. H. Stenning, B. S. Seidel and Y. Senoo	Effect of cascade parameters on rotating stall. N.A.S.A. Memo.3-16-59 W, April, 1959.
3	M. D. Wood, J. H. Horlock and E. K. Armstrong	Experimental investigation of the stalled flow of a single-stage axial-flow compressor. Aero. Quart. Vol.XI, Part 2, May, 1960.
4	A. D. Carmichael	Unsteady flow effects in axial flow compressors and cascades. Cambridge University Thesis, December, 1957.
5	S. R. Montgomery and J. J. Braun	Investigation of rotating stall in a single-stage axial compressor. N.A.C.A. T.N.3823, January, 1957.
6	A. H. Stenning, A. R. Kriebel and S. R. Montgomery	Stall propagation in axial flow compressors. N.A.C.A. T.N.3580, June, 1956.
7	E. L. Costilow and M. C. Huppert	Rotating stall characteristics of a rotor with high hub-tip radius ratio. N.A.C.A. T.N.3518, August, 1955.
8	H. W. Emmons, R. E. Kronauer and J. A. Rocket	A survey of stall propagation - experiment and theory. Trans. A.S.M.E. Vol.81, No.3, pp.409-416, September, 1959.
9	W. D. Rannie and F. E. Marble	Unsteady flows in axial turbomachines. O.N.E.R.A., Comptes Rendus des Journées Internationales Aeronautiques, Part 2, pp.1-21, Paris, May, 1957.
10	W. R. Sears	On asymmetric flow in an axial-flow compressor stage. J. App. Mechanics, pp.57-62, March, 1953.
11	F. E. Marble	Propagation of stall in a compressor blade row. J. Aero. Sciences, Vol.22, No.8, pp.541-554, August, 1955.
12	H. Yeh	An actuator disc analysis of inlet distortion and rotating stall in axial flow turbomachines. J. Aero. Space Sciences, Vol.26, No.11, November, 1959.
13	H. W. Emmons, C. H. Pearson and H. P. Grant	Compressor surge and stall propagation. Paper No.53-A-65 A.S.M.E. Annual Meeting, November, 1953. Also Trans. A.S.M.E., Vol.77, pp.455-467, May, 1955.
14	T. Iura and W. D. Rannie	Experimental investigations of propagating stall in axial flow compressors. Trans. A.S.M.E., Vol.76, pp.463-471, April, 1954.

15/

No.	Author(s)	Title, etc.
15	M. D. Wood	Stall propagation in axial flow compressors. Ph.D. Thesis, Cambridge University, 1955.
16	A. H. Stenning	Stall propagation in compressor blade rows. Readers' Forum, J. Aero. Sciences, Vol.21, October, 1954.
17	D. S. Whitehead	The aerodynamics of axial compressor and turbine blade vibration. Ph.D. Thesis, Cambridge University, 1957.
18	British Association Mathematical Tables	Mathematical Tables Vol.10, Bessel Functions, Part II, (C.U.P., 1952).
19	P. M. Morse	Vibration and sound (2nd Ed., p.449). International series in pure and applied physics. McGraw-Hill, 1948.
20	K. Hayashi	Tafeln der Besselschen etc. (Springer, 1930, Berlin).
21	J. H. Horlock	Axial flow compressors. (Butterworth, 1958).

APPENDIX I/

APPENDIX I

The Conditions Necessary for Perturbation Potential Flow

Euler's equations of motion for steady, inviscid flow in a steadily rotating reference frame, expressed in circular cylindrical co-ordinates are,

$$w_r \frac{\partial w_r}{\partial r} + \frac{w_\theta}{r}\frac{\partial w_r}{\partial \theta} + w_x \frac{\partial w_r}{\partial x} - \frac{(w_\theta + r\Omega)^2}{r} = -\frac{1}{\rho}\frac{\partial p}{\partial r}$$

$$\frac{w_r}{r}\frac{\partial (w_\theta r)}{\partial r} + \frac{w_\theta}{r}\frac{\partial w_\theta}{\partial \theta} + w_x \frac{\partial w_\theta}{\partial x} + 2w_r\Omega = -\frac{1}{\rho r}\frac{\partial p}{\partial \theta}$$

$$w_r \frac{\partial w_x}{\partial r} + \frac{w_\theta}{r}\frac{\partial w_x}{\partial \theta} + w_x \frac{\partial w_x}{\partial x} = -\frac{1}{\rho}\frac{\partial p}{\partial x}.$$

The accelerations relative to inertial space were found by adding to the accelerations seen by the observer in the reference frame rotating at angular velocity, Ω, the Coriolis and centripetal accelerations (see Fig.1(b)).

For w_x write $U(r) + \Delta U(x \tan \beta^* - r\theta, r) + w_x(x,\theta,r)$

and for w_θ write $V^*(r) + \Delta V(x \tan \beta^* - r\theta, r) + w_\theta(x,\theta,r)$.

These are the axial and tangential components of velocity at any point in the flow relative to the rotating stall (see Section 2.1). Substituting the velocity components into the Euler equations and ignoring products of small quantities we obtain,

$$\frac{V^*}{r}\cdot\frac{\partial w_r}{\partial \theta} + U\frac{\partial w_r}{\partial x} - \frac{(V+\Delta V+w_\theta)^2}{r} = -\frac{1}{\rho}\frac{\partial p}{\partial r} \qquad \ldots (I.1)$$

$$w_r\left[\frac{\partial}{\partial r}(rV^*) + 2\Omega r\right] + V^*\frac{\partial}{\partial \theta}(\Delta V + w_\theta) + Ur\frac{\partial}{\partial x}(\Delta V + w_\theta) = -\frac{1}{\rho}\frac{\partial p}{\partial \theta} \qquad (I.2)$$

$$w_r\frac{\partial U}{\partial r} + \frac{V^*}{r}\cdot\frac{\partial}{\partial \theta}(\Delta U + w_x) + U\frac{\partial}{\partial x}(\Delta U + w_x) = -\frac{1}{\rho}\frac{\partial p}{\partial x}. \qquad \ldots (I.3)$$

Now $$\Delta V = \Delta V(x \tan \beta^* - r\theta, r)$$

$$\therefore \frac{\partial \Delta V}{\partial x} = \frac{\partial \Delta V}{\partial (x \tan \beta^* - r\theta)}\cdot \tan \beta^*$$

and $$\frac{1}{r}\cdot\frac{\partial \Delta V}{\partial \theta} = \frac{-\partial \Delta V}{\partial (x \tan \beta^* - r\theta)}$$

In/

In essence, the flow distortion, $(\Delta U, \Delta V)$, outside and downstream of the disc has been assumed to be unaffacted by the perturbations (w_x, w_θ, w_r) caused by the actuator disc.

In equation (I.2)

$$U\frac{\partial \Delta V}{\partial x} + \frac{V^*}{r}\frac{\partial \Delta V}{\partial \theta} = \frac{\partial \Delta V}{\partial (x \tan \beta^* - r\theta)} (U \tan \beta^* - V^*) = 0$$

since $V^*/U = \tan \beta^*$, by definition. A similar result is obtained in equation (I.3), i.e.,

$$U\frac{\partial \Delta U}{\partial x} + \frac{V^*}{r}\frac{\partial \Delta U}{\partial \theta} = 0.$$

Rewriting (I.2) and (I.3)

$$w_r\left[\frac{\partial}{\partial r}(rV^*) + 2\Omega r\right] + V^*\frac{\partial w_\theta}{\partial \theta} + Ur\frac{\partial w_\theta}{\partial x} = -\frac{1}{\rho}\frac{\partial p}{\partial \theta} \qquad \ldots (I.2a)$$

$$w_r\frac{\partial U}{\partial r} + \frac{V^*}{r}\frac{\partial w_x}{\partial \theta} + U\frac{\partial w_x}{\partial x}w_x = -\frac{1}{\rho}\frac{\partial p}{\partial x}. \qquad \ldots (I.3a)$$

The vortex distribution

The flow at stations far removed from the actuator disc ($x = -\infty$ and $x = \infty$) is considered to be in radial equilibrium. If at these stations conditions of radially uniform stagnation enthalpy and entropy exist, the so-called "radial equilibrium equation" may be written as,

$$\frac{d}{dr}(U^2) + \frac{1}{r^2}\frac{d}{dr}\{(rV)^2\} = 0.$$

It is possible to specify any vortex relation $V = V(r)$ and so obtain a solution for $U = U(r)$ using the above equation. The functions $\frac{\partial}{\partial r}(rV^*)$ and $\frac{\partial U}{\partial r}$ can now be found in equations (I.2a) and (I.3a) respectively. However, further development of these equations has been found to be virtually impossible except in the special case of "free-vortex" flow for which a remarkably simple result is obtained.

Assuming free-vortex flow, Vr = constant, it is easily shown that U is constant and so the terms $\left[\frac{\partial}{\partial r}(rV^*) + 2\Omega r\right]$ and $\frac{\partial U}{\partial r}$, in equations (I.2a) and (I.3a) vanish identically. The condition imposed by the assumption of a free-vortex seems to be somewhat restrictive; however, small departures from this condition appear permissible whilst the simplicity of the resulting equations is still preserved.

Consider the absolute tangential velocity distribution

$$V = \frac{\text{constant}}{r} + \bar{v}$$

together/

together with the axial velocity distribution

$$U = \text{constant} + \bar{u}$$

where $\bar{v}$ is any function of r. Then (I.2a) and (I.3a) become,

$$w_r \frac{\partial}{\partial r}(r\bar{v}) + V^* \frac{\partial w_\theta}{\partial \theta} + Ur \frac{\partial w_\theta}{\partial x} = -\frac{1}{\rho}\frac{\partial p}{\partial \theta}$$

$$w_r \frac{\partial \bar{u}}{\partial r} + \frac{V^*}{r}\frac{\partial w_x}{\partial \theta} + U \frac{\partial w_x}{\partial x} = -\frac{1}{\rho}\frac{\partial p}{\partial x}$$

after omitting terms of second order of smallness.

If now $\frac{\bar{v}}{U}$ and $\frac{\bar{u}}{U}$ are made small then the terms $w_r \frac{\partial}{\partial r}(r\bar{v})$ and $w_r \frac{\partial \bar{u}}{\partial r}$ can be ignored as being of the second order of smallness.

Hence,

$$V^* \frac{\partial w_\theta}{\partial \theta} + Ur \frac{\partial w_\theta}{\partial x} = -\frac{1}{\rho}\frac{\partial p}{\partial \theta} \qquad \ldots (I.2b)$$

$$\frac{V^*}{r}\frac{\partial w_x}{\partial \theta} + U \frac{\partial w_x}{\partial x} = -\frac{1}{\rho}\frac{\partial p}{\partial x}. \qquad \ldots (I.3b)$$

By cross differentiating equations (I.1), (I.2b) and (I.3b) in pairs the pressure terms can be eliminated to give the Helmholtz vorticity equations,

$$\frac{V^*}{r}\frac{\partial \xi}{\partial \theta} + U\frac{\partial \xi}{\partial x} = \frac{2V}{r^2}\frac{\partial \Delta V}{\partial \theta} \qquad \ldots (I.4)$$

$$\frac{V^*}{r}\frac{\partial \eta}{\partial \theta} + U\frac{\partial \eta}{\partial x} = \frac{2V}{r}\left(\frac{\partial \Delta V}{\partial x} - \xi\right) \qquad \ldots (I.5)$$

$$\frac{V^*}{r}\frac{\partial \zeta}{\partial \theta} + U\frac{\partial \zeta}{\partial x} = 0 \qquad \ldots (I.6)$$

where ξ, η and ζ are the vorticity components due to the perturbation velocities alone along the axial, tangential and radiation directions respectively, i.e.,

$$\xi = \frac{1}{r}\left\{\frac{\partial}{\partial r}(rw_\theta) - \frac{\partial w_r}{\partial \theta}\right\}$$

$$\eta = \frac{\partial w_r}{\partial x} - \frac{\partial w_x}{\partial r}$$

$$\zeta = \frac{1}{r}\left\{\frac{\partial w_x}{\partial \theta} - \frac{\partial (rw_\theta)}{\partial x}\right\}.$$

The/

The LHS of equations (I.4), (I.5) and (I.6) can be shown to be the product of the resultant undisturbed velocity $W = \sqrt{U^2 + V^{*2}}$ and the convective rate of change of perturbation vorticity along lines at the downstream ($x = \infty$) relative flow angle, $\beta_2^* \equiv \tan^{-1} \frac{V_2^*}{U}$, for a constant radius. With s as the distance along the line, equation (I.4), for example, can be written as,

$$W \frac{d\xi}{ds} \equiv U \frac{d\xi}{dx} \equiv \frac{V^*}{r} \frac{d\xi}{d\theta} = \frac{2V}{r^2} \frac{\partial \Delta V}{\partial \theta} .$$

Now because of the presence of the ΔV component of the self-induced distortion (see Section 2.1) which originates, incidentally, in the centripetal acceleration term of equation (I.1), a convective rate of change of ξ and η is apparent (I.4) and (I.5).

In equation (I.6), $U \frac{d\zeta}{dx} = 0$ and ζ is constant or zero; ζ is taken to be zero for reasons stated above.

The RHS of equations (I.4) and (I.5) can be written respectively as,

$$-\frac{2V}{r} \frac{\partial \Delta V}{\partial (x \tan \beta_2^* - r\theta)} ,$$

and

$$\frac{2V}{r} \tan \beta_2^* \frac{\partial \Delta V}{\partial (x \tan \beta_2^* - r\theta)} .$$

Both of these expressions are zero when either:-

(i) $r \to \infty$; in the limit for finite blade height this reduces to the infinite actuator strip employed by Yeh[12] as the flow model, or,

(ii) $V = 0$; since the self-induced distortion supposed present only aft of the disc, the condition $V = 0$ is only required at stator exit.

Neither of these two conditions is particularly satisfactory. The above expressions can, however, be reduced to the second order of smallness by means of the following device. Consider the expression,

$$U \frac{d\xi}{dx} = -\frac{2V}{r} \frac{\partial \Delta V}{\partial (x \tan \beta_2^* - r\theta)} \equiv -\frac{2V}{r} (\Delta V') .$$

Integrating,

$$\Delta\xi = -\frac{2V}{U} \left(\frac{r_o}{r} \right) \left(\frac{\Delta x}{r_o} \right) (\Delta V') \qquad \ldots (I.7)$$

where Δx is a representative axial distance measured from the origin in which the change of vorticity, $\Delta\xi$ occurs. All perturbation velocities, it may be argued, may be represented by functions of the form

$e^{-mx+in\theta}$, $(x > 0)$, which is not necessarily a potential function.

Then, if (for example) $w_x \propto e^{-mx+in\theta}$

$$\frac{w_x}{w_{x_{max}}} /$$

$$\frac{w_x}{w_{x_{max}}} = \frac{e^{-m\Delta x+in\theta}}{e^{in\theta}} = e^{-1} \quad \text{(say)}$$

where Δx is an axial distance in which the axial velocity perturbation has decayed to $1/e$ of its original value

$$\therefore \quad m\Delta x = 1.$$

Inspecting orders of magnitude in (I.7)

$$\Delta\xi = -\frac{2V}{U}\left(\frac{r_o}{r}\right)\left(\frac{\Delta x}{r_o}\right)(\Delta V'), \quad \text{for large } m$$

$$\delta^2 = \qquad 1 \qquad \delta \qquad 1$$

i.e., with the assumptions of large m and small absolute exit flow angle, the vorticity change must be of the second order of smallness. Hence

$$\xi = \eta = \zeta = 0$$

which is the potential solution in Section 3. Finally from Fig.6, large values of (mr_o) occur, in general, for a large number of stall cells n. (The higher roots of the boundary solution give large mr_o for small n but these may be of less importance than the primary root.)

The conditions necessary for downstream perturbation potential flow are a large number of stall cells together with a small absolute exit flow angle. An implicit assumption in the above analysis is that the exit flow is close to a free vortex distribution. If the exit flow angle is zero, however, the necessity of restricting the analysis to a large number of stall cells vanishes.

APPENDIX II/

APPENDIX II

Asymptotic Solution of Bessel Function Equation, $f(\mu) = 0$

$$f(\mu) = \frac{J'_n(\mu)}{Y'_n(\mu)} - \frac{J'_n\left(\frac{r_i}{r_o} \cdot \mu\right)}{Y'_n\left(\frac{r_i}{r_o} \cdot \mu\right)} .$$

In the above equation for large values of μ and with $r_i/r_o = \frac{1}{2}$ the second term becomes very small compared with the first term. The second term may then be neglected and the result is $J'_n(\mu) = 0$.

Now $$J'_n(\mu) = \tfrac{1}{2}[J_{n-1}(\mu) - J_{n+1}(\mu)] = 0$$

$$\therefore \; J_{n-1}(\mu) = J_{n+1}(\mu) .$$

Some values of J are available in the tables[20], for $\mu = 50$ and 100 and $n = 1, 2, 3, \ldots 100+$ which can be used to extend somewhat the solutions of Fig.6 (for $r_i/r_o = \frac{1}{2}$ only). These are shown in Fig.7 indicating sufficiently that for large values of n,

$$\frac{n}{\mu} = q \frac{r}{r_o} \rightarrow 1 \quad \text{for all roots.}$$

WS

FIG. 1(a)

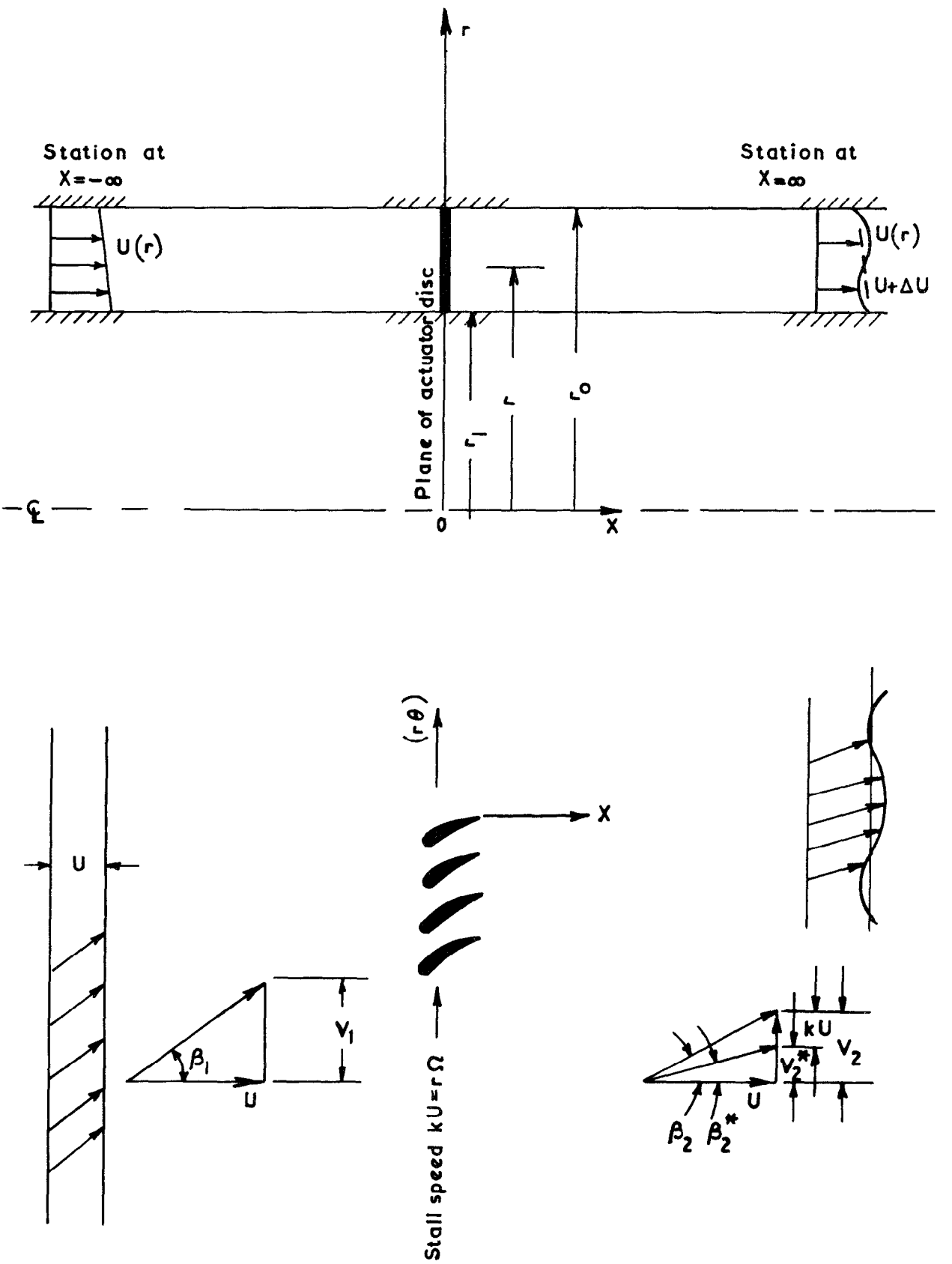

Velocity diagrams and co-ordinate axis.

FIG. 1 (b)

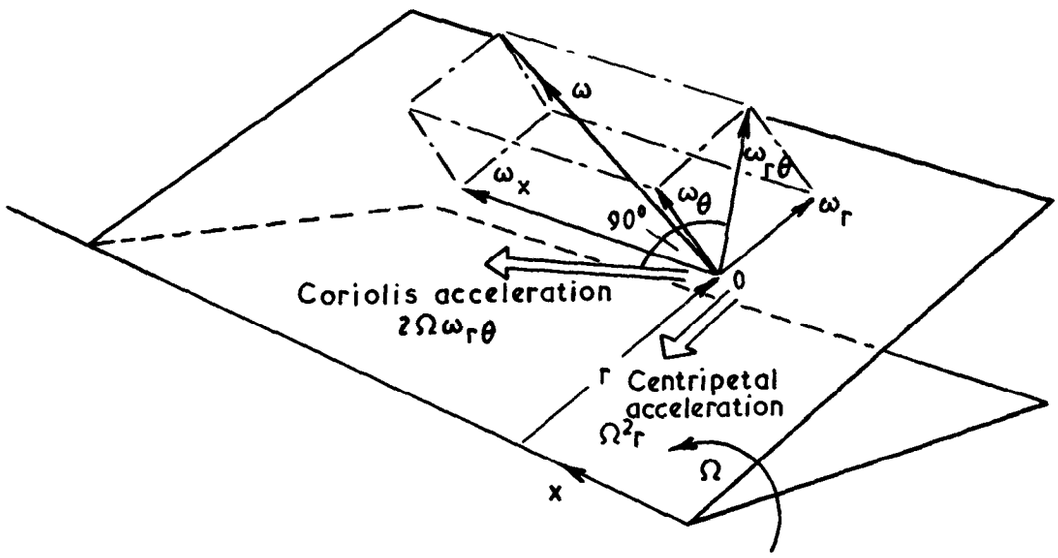

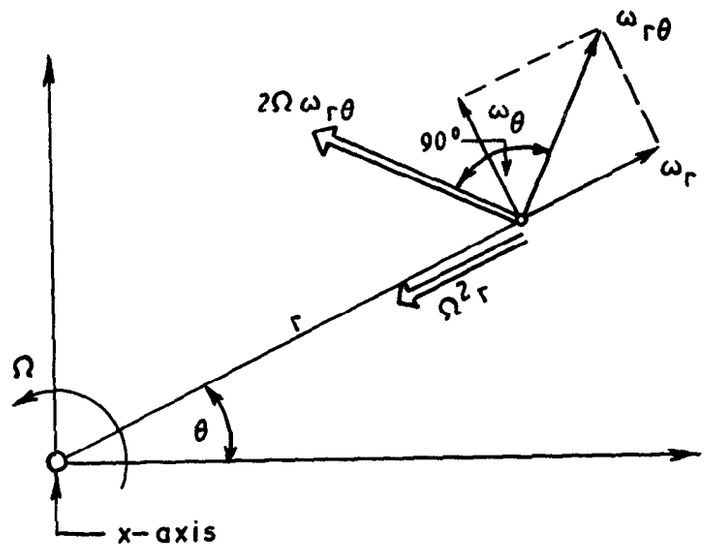

Components of velocity relative to a steadily rotating reference frame and the additional acceleration components.
(See Appendix I)

FIG. 2

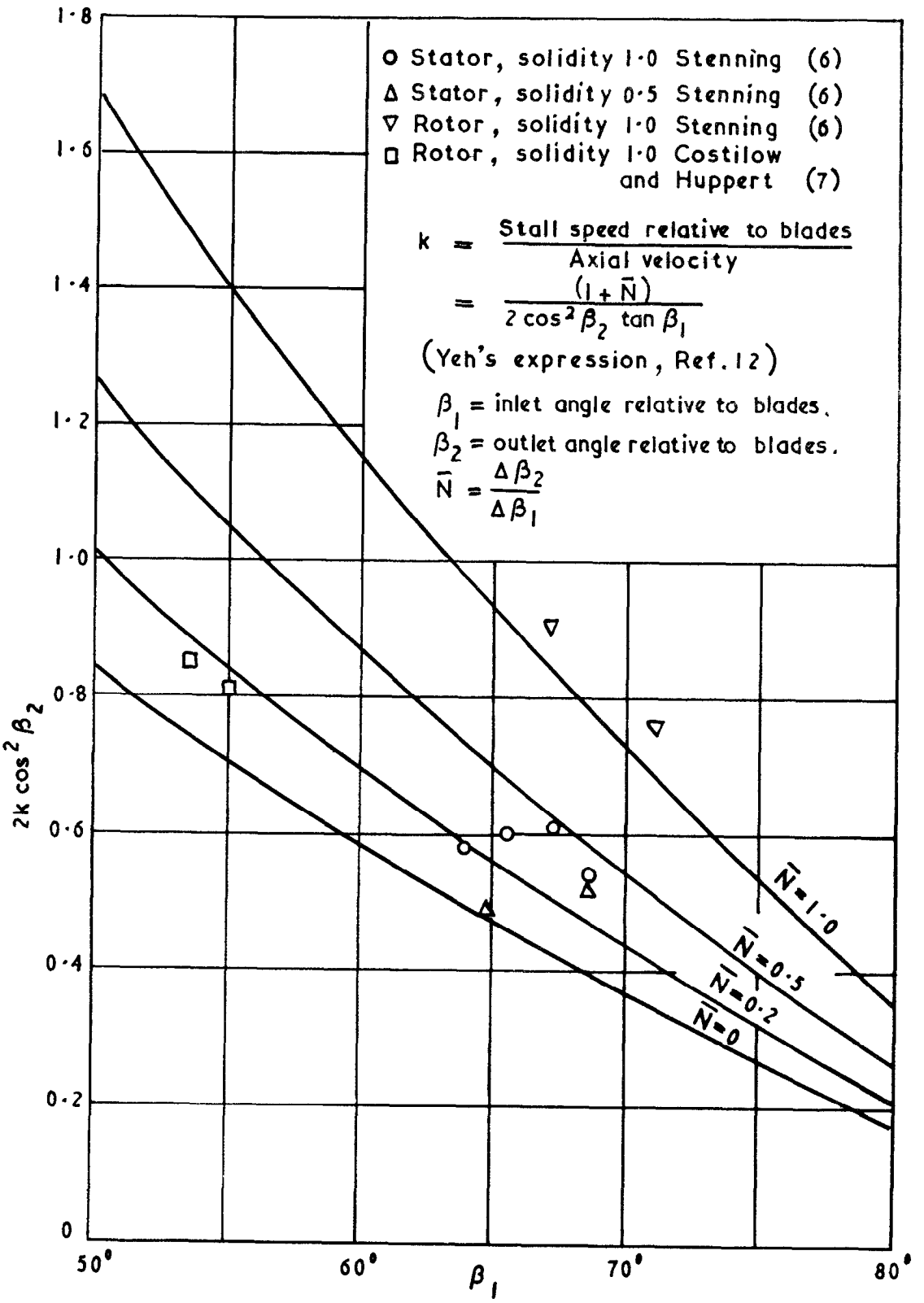

Comparison of theoretical velocity of propagation of "incipient stall" with experiment. (After Yeh)

FIG. 3

(a) Variation of necessary M with b_1 and wave parameter, q for $b_2=0$, $N=0$, $\bar{\omega}=0$.

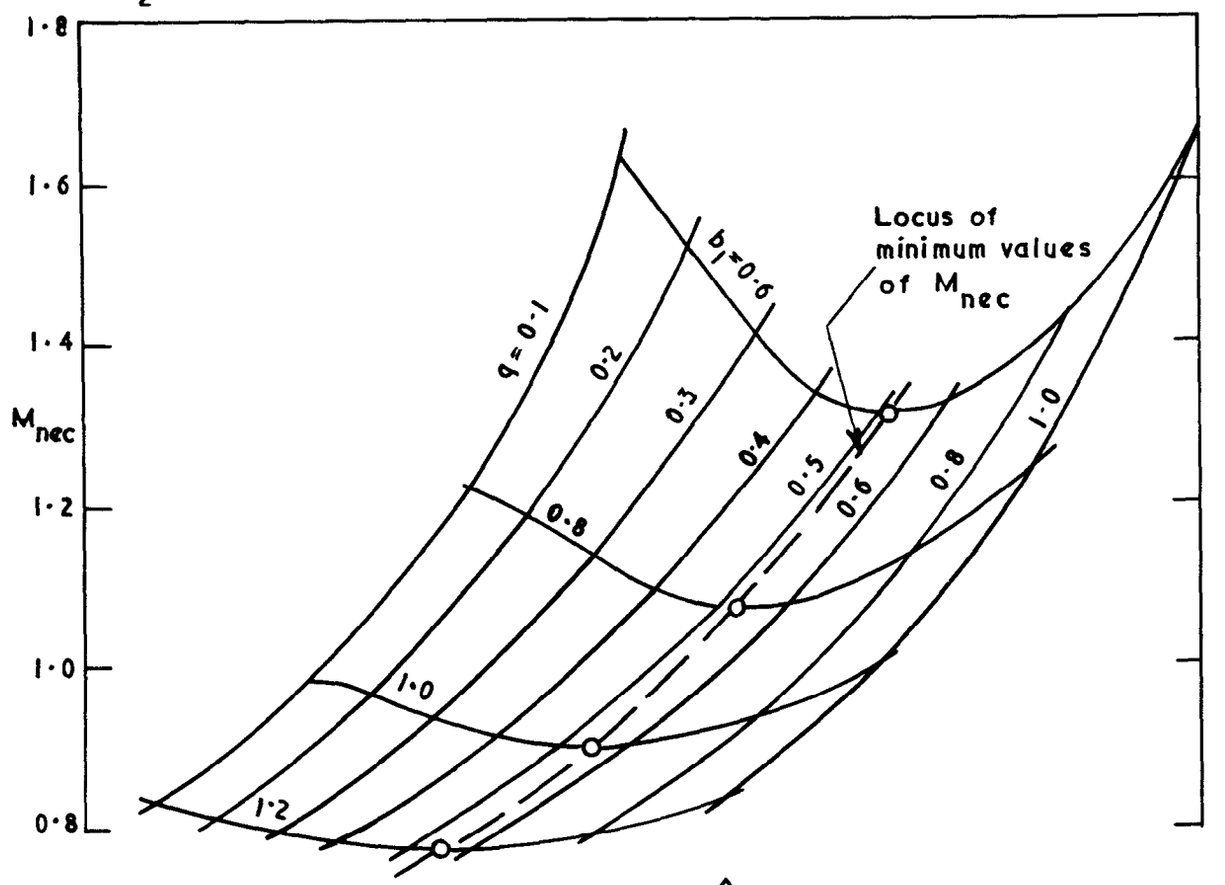

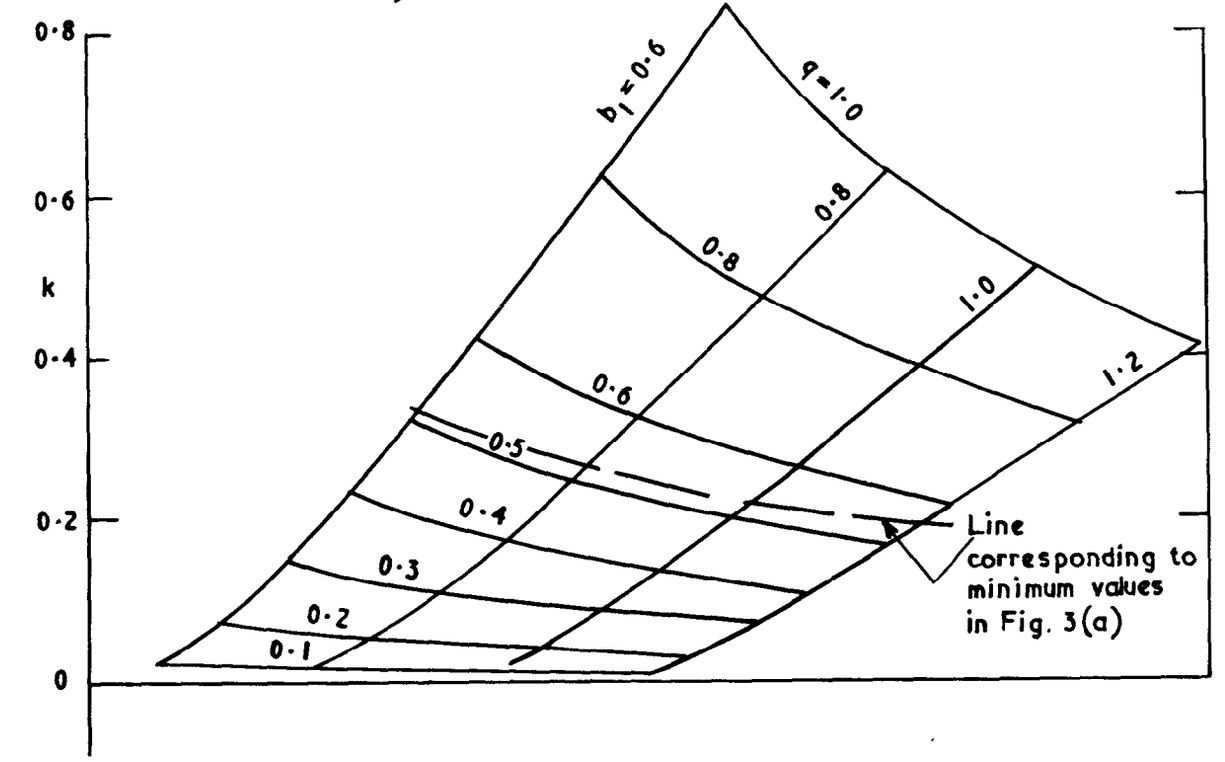

(b) Values of k corresponding to necessary M values.

FIG 4

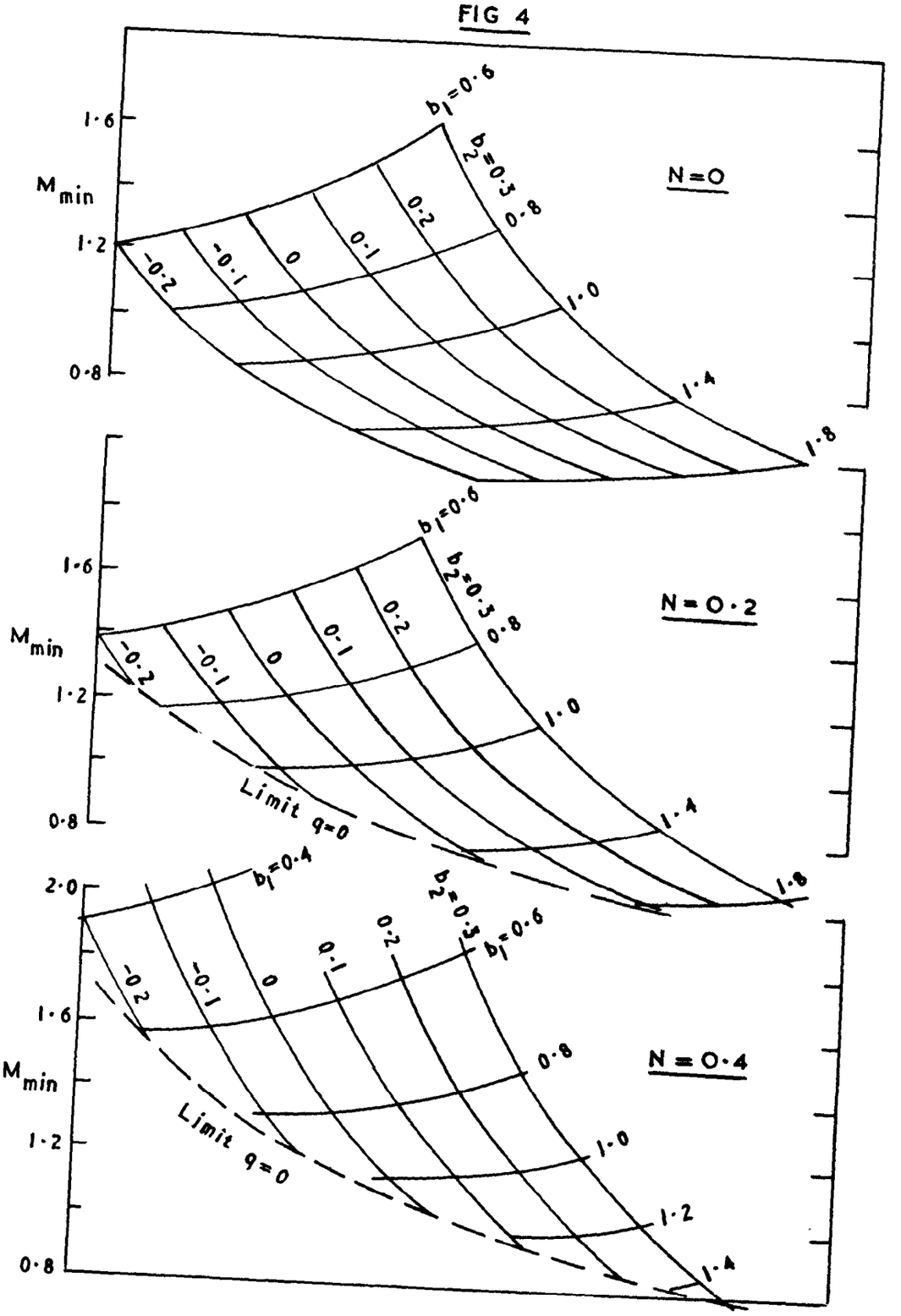

Values of M_{min} against b_1 and b_2 for various N values.

FIG. 5.(a)

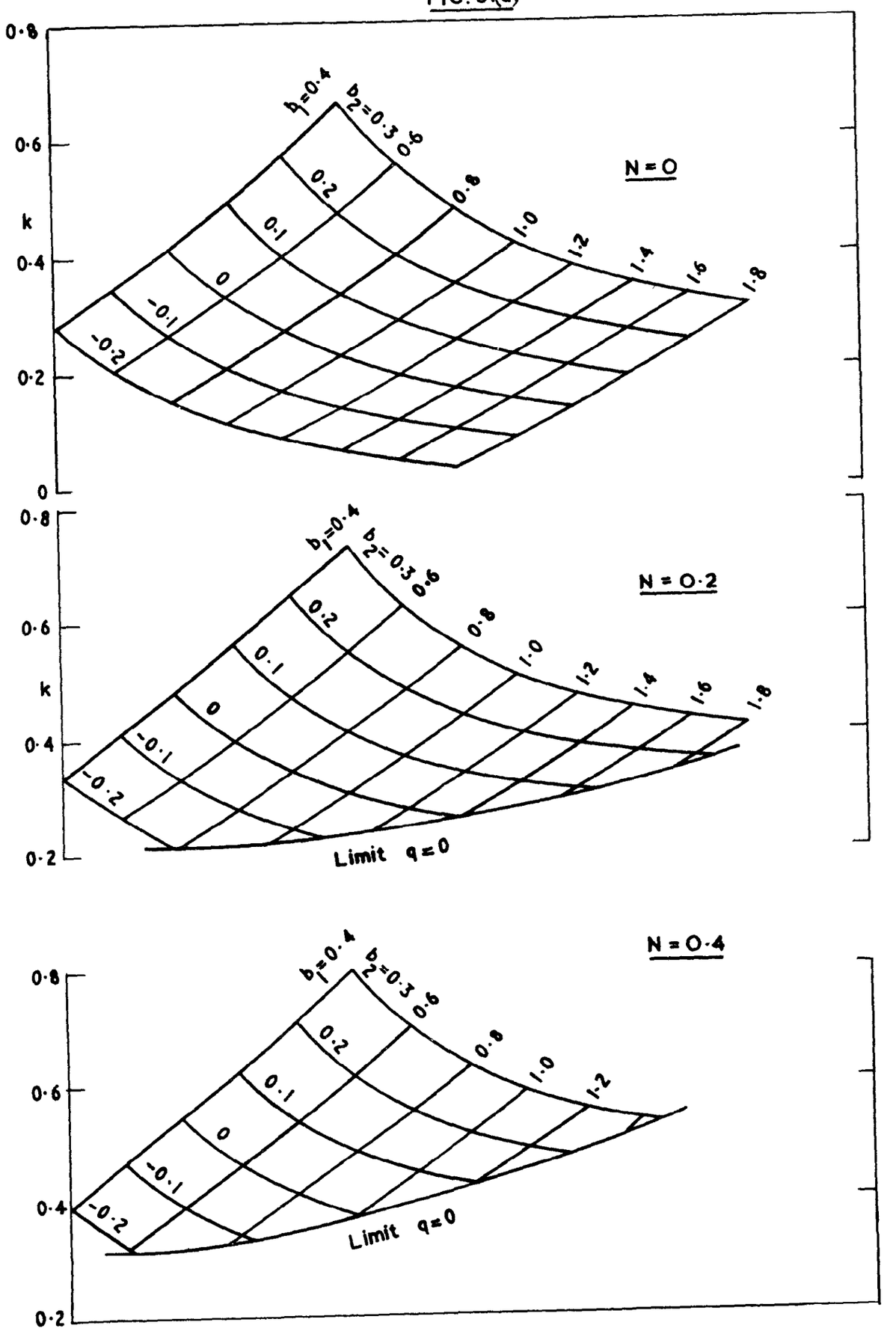

Values of k corresponding to M_{min} against b_1 and b_2

FIG. 5(b)

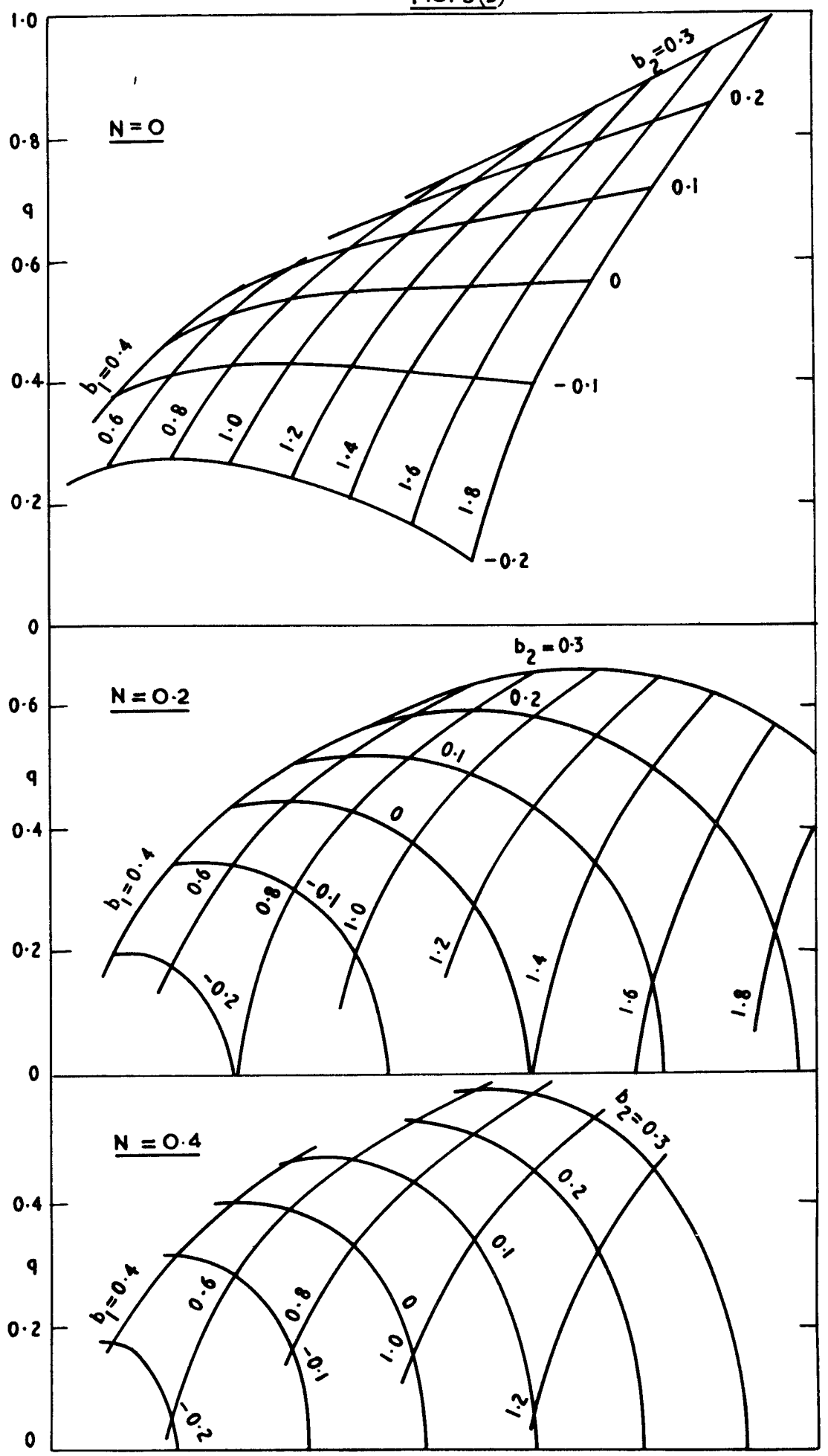

Values of q corresponding to M_{min} against b_1 and b_2

FIG. 6

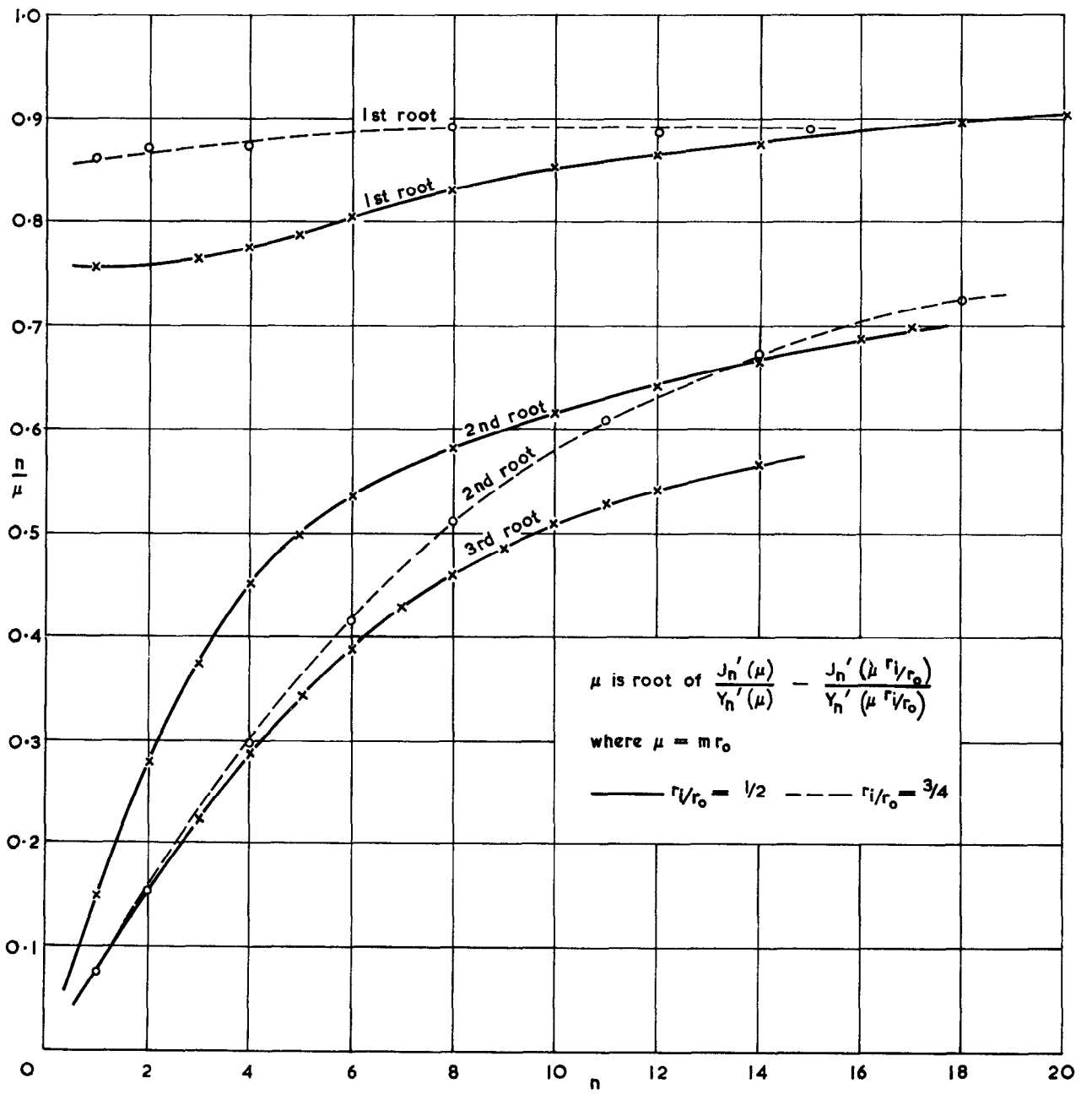

Roots of boundary Bessel-function equation

FIG. 7.

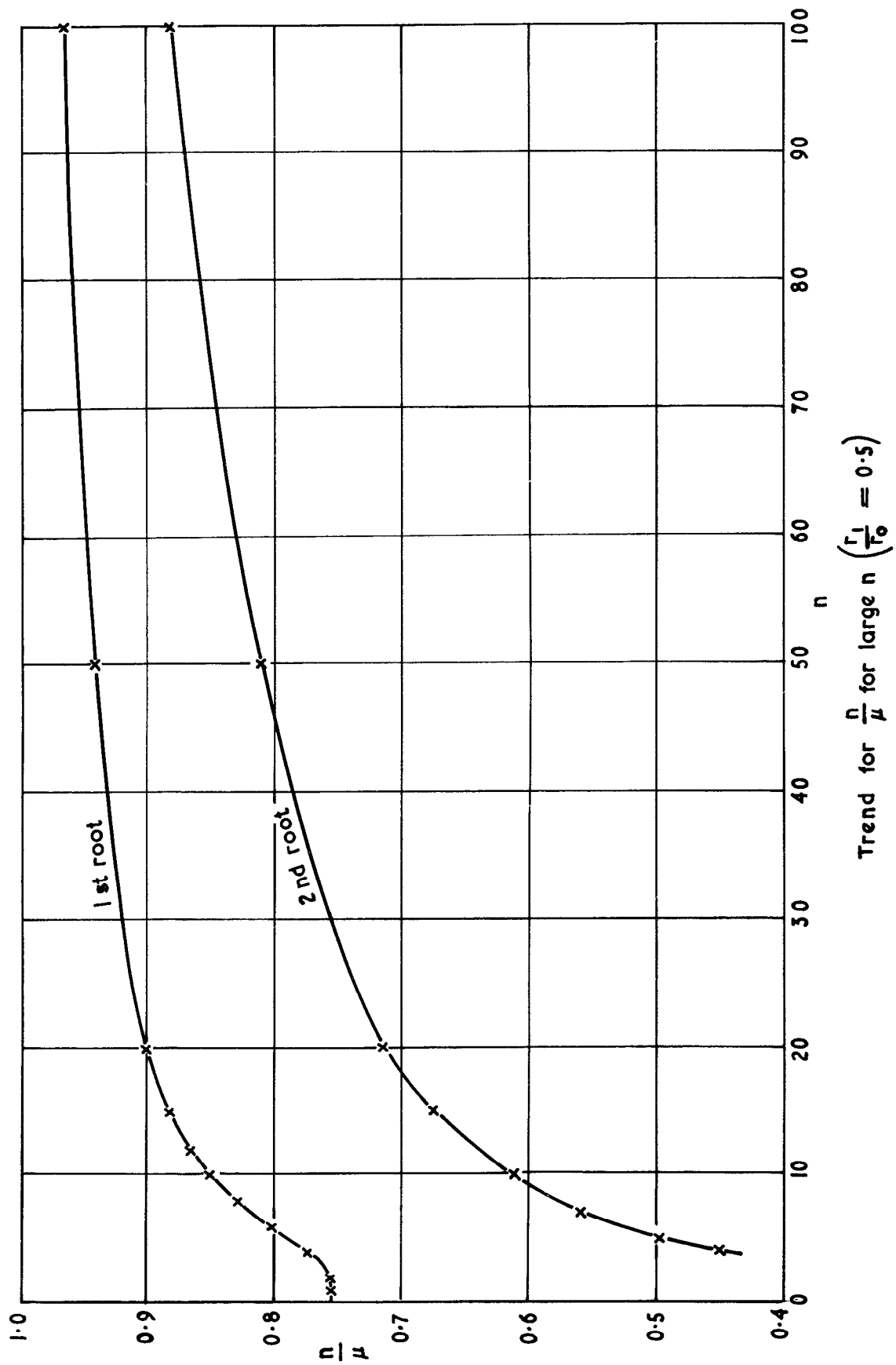

DS 66802/1/Wt.58 K4 8/62 XL/CL

A.R.C. C.P. No.609. May, 1961.
Dixon, S. L. - Univ. of Liverpool

SOME THREE-DIMENSIONAL EFFECTS OF ROTATING STALL

A small perturbation analysis of rotating stall in inviscid, incompressible flow is developed from an analysis of Yeh. An isolated blade row is considered having a blade height which is not small compared to the mean radius. A criterion is derived for the occurrence of rotating stall, the speed of stall propagation and the possible number of stall cells involved. From this the frequency of circumferential flow disturbances can be obtained. Application of the analysis to an example is given. Possible explanations are suggested for the observed changes in number of stall cells.

A.R.C. C.P. No.609. May, 1961.
Dixon, S. L. - Univ. of Liverpool

SOME THREE-DIMENSIONAL EFFECTS OF ROTATING STALL

A small perturbation analysis of rotating stall in inviscid, incompressible flow is developed from an analysis of Yeh. An isolated blade row is considered having a blade height which is not small compared to the mean radius. A criterion is derived for the occurrence of rotating stall, the speed of stall propagation and the possible number of stall cells involved. From this the frequency of circumferential flow disturbances can be obtained. Application of the analysis to an example is given. Possible explanations are suggested for the observed changes in number of stall cells.

A.R.C. C.P. No.609. May, 1961.
Dixon, S. L. - Univ. of Liverpool

SOME THREE-DIMENSIONAL EFFECTS OF ROTATING STALL

A small perturbation analysis of rotating stall in inviscid, incompressible flow is developed from an analysis of Yeh. An isolated blade row is considered having a blade height which is not small compared to the mean radius. A criterion is derived for the occurrence of rotating stall, the speed of stall propagation and the possible number of stall cells involved. From this the frequency of circumferential flow disturbances can be obtained. Application of the analysis to an example is given. Possible explanations are suggested for the observed changes in number of stall cells.

Printed and published by
HER MAJESTY'S STATIONERY OFFICE

To be purchased from
York House, Kingsway, London, W.C.2
423 Oxford Street, London W.1
13A Castle Street, Edinburgh 2
109 St. Mary Street, Cardiff
39 King Street, Manchester 2
50 Fairfax Street, Bristol 1
35 Smallbrook, Ringway, Birmingham 5
80 Chichester Street, Belfast 1
or through any bookseller

Printed in England

S.O. Code No. 23-9013-9